

# Synthesis of Iron Nanoparticles Using *Psidium guajava* Leaf Extract and It's Role in Crystal Violet Dye Removal

Sai Gowtham Allu<sup>1</sup>, Thanusha Punugoti<sup>2</sup>, Mathala Christopher Marlowe<sup>3</sup> and Meena Vangalapati<sup>4\*</sup>

<sup>1</sup>Master of Technology, Department of Chemical Engineering, AUCE(A), Visakhapatnam, 530003, AP, India.

<sup>2,3</sup>Bachelor of Technology, Department of Mechanical Engineering, AUCE(A), Visakhapatnam, 530003, AP, India.

<sup>4\*</sup>Professor, Department of Chemical Engineering, AUCE(A), Visakhapatnam, 530003, AP, India

## Abstract

Green process techniques have been favored in recent years due to their influence on wastewater removal, and they are being emphasized in the advancement of nanotechnology. Eco-friendliness and abundance in nature make green materials preferable in nanoscience. *Psidium guajava* leaf extract was employed in this study to manufacture ecologically friendly iron nanoparticles. The FeNPs are used in the removal of Crystal violet dye which is used in textile industries and as a disinfectant. It is known to cause animal carcinogenicity and permanent skin coloring in humans when in Contact. There is a need for removal from natural bodies frequently used by living beings. FTIR, SEM, XRD, and EDX are used in the characterization of iron NPs from *Psidium guajava*, and the benefits of green synthesis are observed. Adsorption studies in batch format are used for the removal of a textile dye from an aqueous solution. The Studies are done considering parameters of Contact time, pH, Initial dye concentration, adsorbent dosage, and temperature. The removal efficiency obtained by plant-synthesized Iron NPs for Crystal violet dye is around 99%. We attempted to create an eco-friendly, less energy-intensive, and more effective approach for textile dye degradation.

**Keywords:** Crystal Violet Dye; FeNPs; *Psidium guajava*; SEM; XRD; FTIR; Adsorption

\*Correspondence to: Meena Vangalapati, Department of Chemical Engineering, Andhra University, Visakhapatnam, Andhra Pradesh, India; E-mail: [meenasekhar2002@yahoo.com](mailto:meenasekhar2002@yahoo.com)

**Citation:** Allu SG, Punugoti T, Marlowe MC, Vangalapati M (2022) Synthesis of Iron Nanoparticles Using *Psidium guajava* Leaf Extract and It's Role in Crystal Violet Dye Removal. *Nanotechnol Nanomater Res*, Volume 3:2. 116. DOI: <https://doi.org/10.47275/2692-885X-116>

**Received:** October 04, 2022; **Accepted:** December 23, 2022; **Published:** December 26, 2022

## Introduction

With the Increase in Pollution and Global Warming, the need for sustainability of the planet has become the primary priority. Greener methods are found to be less energy-consuming abundant, eco-friendly, and less toxic compared to the chemical and physical methods for synthesizing nanoparticles [1]. Iron Nanoparticles are synthesized using *Psidium guajava* as they possess anti-bacterial and eco-friendly compared to the chemical and mechanical methods which may be toxic and highly energy consuming.

*Psidium guajava* also called guava is known for its anti-diabetic, anti-diarrhea, anti-mutagenic and anti-microbial properties and has also been found to be safe in toxicity studies. Nanoparticles are preferred for dye removal due to the unique properties they possess. Nanoparticles are known for their high surface area, chemical reactivity, and mechanical strength. *Psidium guajava* is used in the synthesis of Iron Nanoparticles. FeNPs are known for their increased stability and positively affecting cells. FeNPs combat harmful dyes and also have anti-bacterial activity.

The Crystal violet dye, an alkaline dye of organic salts from the triphenylmethane group is used in gram staining, Dyeing ink, and Antibacterial and Antifungal agent. It is also used in fields of the textile manufacturing and the cosmetic industry, as components of ink in printers and forensic studies, and as a marker during surgeries. It is known to cause animal carcinogenicity, and permanent skin coloring

when in contact with a tissue. In some countries, Crystal violet dye is banned for human usage. The Gram stain is a differential stain that distinguishes gram-positive and gram-negative bacteria based on the type of bacterial cell wall. To remove a textile dye (Crystal violet) from an aqueous solution, the Adsorption process was used. In this paper, The present work studies the synthesis of FeNPs using green synthesis and various parameters including dosage, pH, concentration, temperature, and contact time used during the degradation of Crystal violet dye.

## Materials and Methods

### Preparation of *Psidium guajava* Leaves Extract

The leaves of *Psidium guajava* were harvested. In a conical flask, ten grams of leaves are placed. Fill the flask with 100ml of deionized water. Simultaneously, Individual leaf extracts were made. For 10 minutes, the mixture is heated to 80°C, then it is cooled to room temperature and filtered. When kept at 40°C, the filtrate can be utilized for a week.

### Synthesis of Iron Nanoparticles

In a 1:1 ratio to the filtrate, 8.11g of FeCl<sub>3</sub> granulates are added to 500 ml of *Psidium guajava* leaf extract. A mechanical stirrer is used to agitate the liquid at room temperature until a black precipitate form. The formation of a black precipitate indicates the reduction of Fe<sup>+2</sup> ions. [2]. The precipitate is then dried in a vacuum at 65°C after centrifuging at 5000 rpm for 20 minutes [3-8].



Figure 1: *Psidium guajava* leaves.

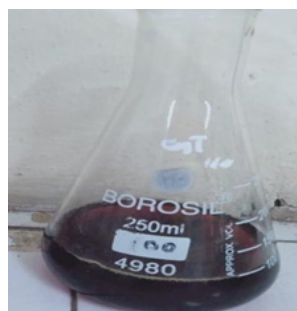


Figure 2: *Psidium guajava* extract.

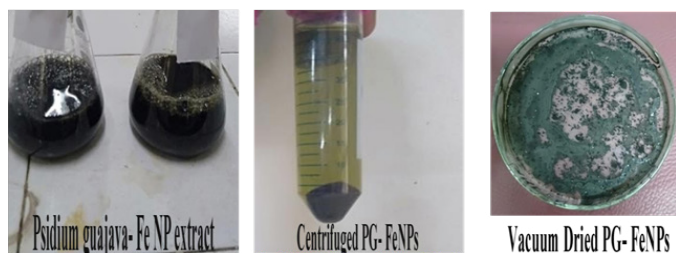


Figure 3: *Psidium guajava*-Fe NP extract, Centrifuged PG-FeNPs and vacuum dried PG-FeNPs.

### Characterization of PG-FeNPs

Scanning Electron Microscope (SEM) provides the topography, morphology and composition of the materials. It also determines the size of the particles using Debye-Scherrer formula. SEM images were taken using a Zeiss scanning electron microscopy operating at 10kV.

X-Ray Diffraction (XRD) is used to determine the crystalline nature of the compound. XRD analysis pattern is done for *Psidium guajava* FeNPs in between 0-80°. Sharpness in the peaks determines the crystalline nature of the compound.

FTIR analysis (Bruker optics, Germany, Tensor 27) is done before and after for FeNPs. The Analysis is done in the range of 400-4000  $\text{cm}^{-1}$ . FTIR analysis is done to determine the functional groups present in the compound. FTIR analysis (Bruker optics, Germany, Tensor 27) is done before and after for FeNPs. The Analysis is done in the range of 400-4000  $\text{cm}^{-1}$ . FTIR analysis is done to determine the functional groups present in the compound.

EDX spectroscopy gives the elemental analysis or chemical composition of the compound.

## Results and Discussion

### Scanning Electron Microscope (SEM)

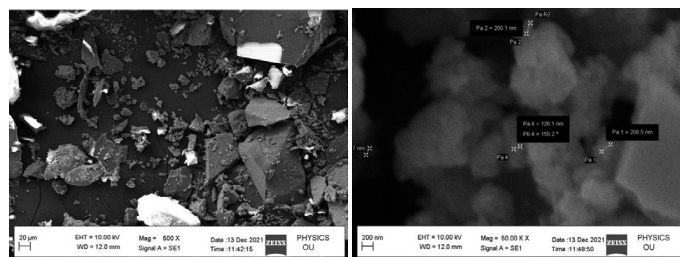


Figure 4: SEM images of PG-FeNPs of (a) 20µm magnification (b) 200µm magnification.

The SEM (Scanning Electron Microscope) picture shows the minute structures and various sizes of PG-FeNP in great detail. For the best imaging, it offers consistent and high-resolution probe currents. The generated nanoparticles have a size between 159.3 and 205.6 nm. The Nanoparticles display a sporadic FeNP formation with various forms and void development [5,9 and 10]. Agglomeration of created nanoparticles may be seen in the aforementioned figures [5,11]. NPs in spherical shape were agglomerated with iron nanoparticles, as demonstrated by green synthesis [4,12-16].

### Energy Dispersive X-ray Spectroscopy (EDX)

According to the elemental analysis of EDX, Cl, Fe, O, and C elements are present. EDX showed intense peaks for C, O and Fe indicating the major components used in the synthesis of iron nanoparticles [11,13, and 14]. Fe indicates the presence of iron nanoparticles, whereas leaf extract contains C, and O. Water and flavonoid content are the sources of oxygen molecules [13]. The polyphenol groups and other C-containing compounds in *Psidium guajava* extracts are responsible for the presence of C signals [11]. The precursors utilised in the synthesis of PG-FeNPs are what cause the presence of Cl in addition to the Fe elemental composition [10]. The elemental composition of Zn, Fe, and O was found in Zn-Fe NPs with *Psidium guajava* [7].

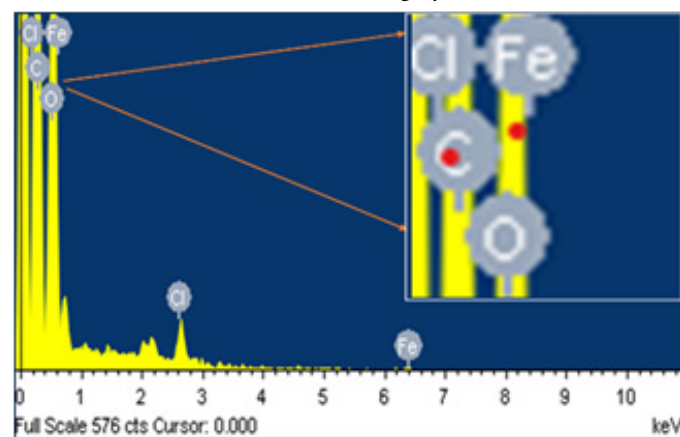


Figure 5: EDX of PG-FeNPs.

### X-Ray Diffraction (XRD)

Iron nanoparticles appear to be crystalline in form, according to the XRD Pattern [11]. The  $2\theta$  values of the peaks for *Psidium guajava* Fe NPs are obtained at 10.92°, 17.94°, 22.31°, 29.52°, 38°, 42°, 43.8°, 48°, 55°, 60.8°, 68° and 77° [13,17]. Huang showed that iron nanoparticles produced using tea extracts had  $2\theta$  values of 20.35°, 35.45°, 35.68°, and 44.9° and are amorphous in form. Similarly, when using Avicenna



marina flower extract in a plant-mediated synthesis, an XRD pattern clearly demonstrates how nanoparticles are created by the reduction of metal ions, and peaks support the structure's crystallinity [16].

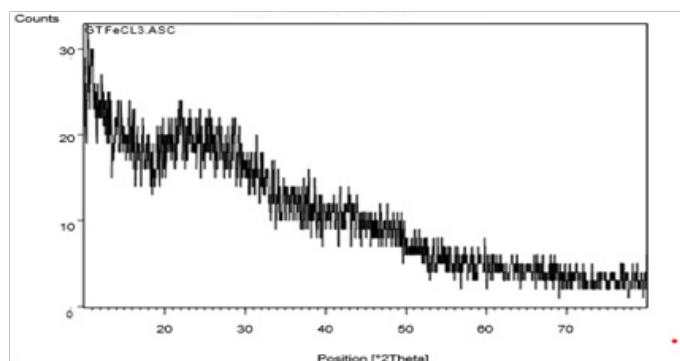


Figure 6: XRD of PG-FeNPs Intensity vs 2θ.

#### Fourier Transforms and Infrared Radiation (FTIR)

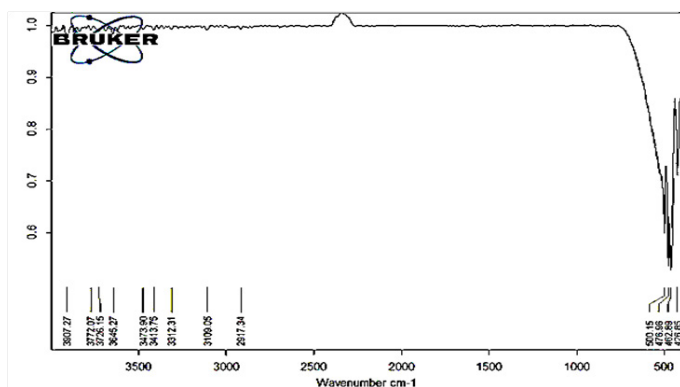


Figure 7: Above shows the FTIR analysis Iron Nanoparticles before treatment with *Psidium guajava*.

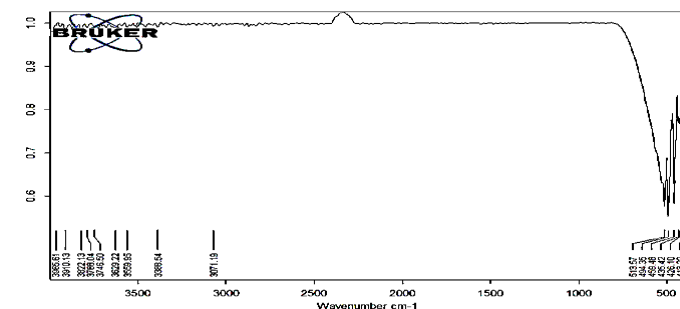


Figure 8: Above shows the FTIR analysis Iron Nanoparticles after treatment with *Psidium guajava*.

FeNPs' FTIR bands before and after *Psidium guajava* treatment are shown in Figure 7 and Figure 8. The presence of Fe-O functional groups is responsible for the peaks between  $400\text{ cm}^{-1}$  and  $510\text{ cm}^{-1}$ . Due to the presence of hematite nanoparticles, the peak at  $470\text{ cm}^{-1}$  is present. [13,15, and 17]. The peaks at  $2900\text{ cm}^{-1}$  in aliphatic hydrocarbons indicate the vibrations of C-H and C-H<sub>2</sub> [9]. O-H stretching of polyphenol compounds causes peaks to appear between  $3300\text{ cm}^{-1}$  and  $3500\text{ cm}^{-1}$  [4-6,9, and 15]. Similarly, at  $3416\text{ cm}^{-1}$ , OH stretching is produced for the Green Synthesis of NPs utilising *Pheonix dactylifera* [12]. The band undergoes a shift from  $3413\text{ cm}^{-1}$  to  $3388.54\text{ cm}^{-1}$  and becomes broader upon interaction with iron salts [12]. The reduction of ferric chloride and its aqueous phase is mostly due to

phenolic chemicals [18]. Plant extracts include phenolic compounds, which are well-known for functioning as reducing agents. [6,9, and 11]. They additionally serve as stabilizers by strengthening connections with water molecules [5,12, and 13].

To investigate the impact of different parameters on the removal of Crystal violet from the aqueous solution (made in the lab), experimental data is obtained in a batch mode of operation utilising PG- FeNP as an adsorbent. After conducting an experimental examination of the impact of several factors on the adsorption of crystal violet, it was attempted to conceptually support the findings. The current study conducts a number of different experimental runs.

#### Effect of Contact Time(t)

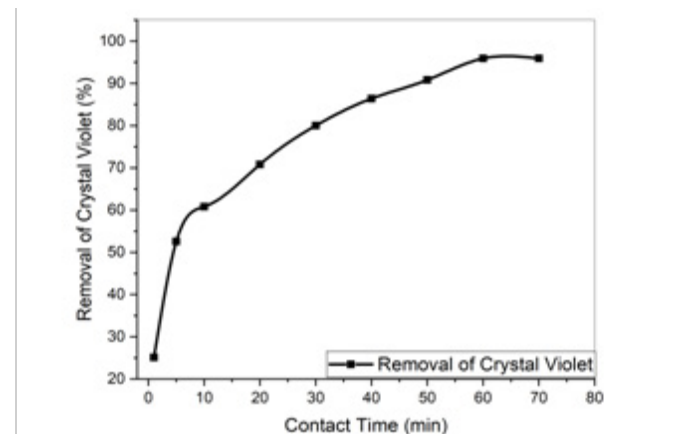


Figure 9: Effect of Contact time of PG-FeNPs on Crystal Violet dye.

Time course profiles for the adsorption of crystal violet solutions are displayed for the time intervals of 1, 5, 10, 20, 30, 40, 50, 60, and 70 min. The amount of dye removal rises as contact duration increases [9]. The graph shows that Crystal Violet PG-FeNPs adsorption requires a contact period of 60 minutes to reach adsorption equilibrium. After 60 minutes, there is no discernible change in the dye concentration with increasing contact time. The contact period's equilibrium duration of 60 min has been chosen in order to facilitate future research on the adsorption of PG-FeNP with other parameters. The gradual shift in dye removal percentage after 60 minutes is caused by a decreasing concentration gradient and diffusion rate with an increase in contact duration [8].

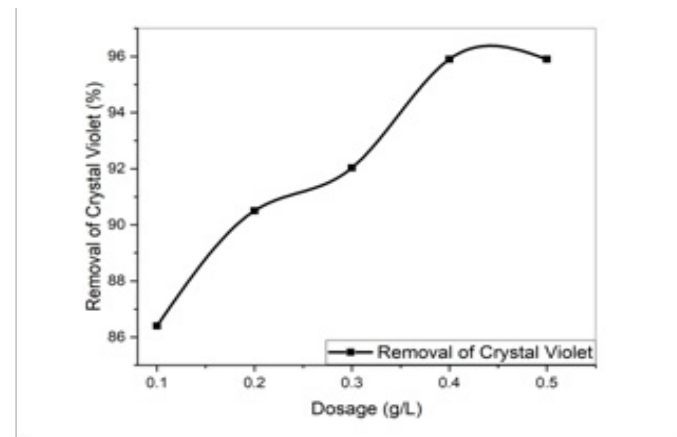


Figure 10: Effect of adsorbent dosage on Crystal Violet dye using PG-FeNPs.



### Effect of Adsorbent Dosage(W)

The impact of adsorbent dose is investigated for the removal of crystal violet dye maintaining other parameters constant. The graph demonstrates that the amount of dye removed rises when the adsorbent dose is increased. It is explained by the increase in crystal violet removal that occurs when the adsorbent dosage is increased from 0.1 to 0.5g. PG-FeNPs were used to boost the elimination percentage for a 20 mg/L dye solution from 86.4% to 91.2% and a maximum of 96% is obtained for 40mg/L dosage. An increase in surface area and a large number of readily available sorption sites allow CV Dye to be absorbed [7,19].

### Effect of Solution pH

Adsorption is affected by a number of factors, including pH. From the graph, it can be seen that as the pH rises from 5 to 7, the percentage of dye removed increases. However, when the pH rises further, up to 9, the percentage of dye removal decreases. As a result, the optimal pH is considered to be 7. Less adsorption occurs at lower pH levels as a result of the hydrogen ions' competition with the crystal violet ions. With the increase in pH, there is an increase in OH<sup>-</sup> ions leading to electrostatic attraction with Crystal violet ions [20-22].

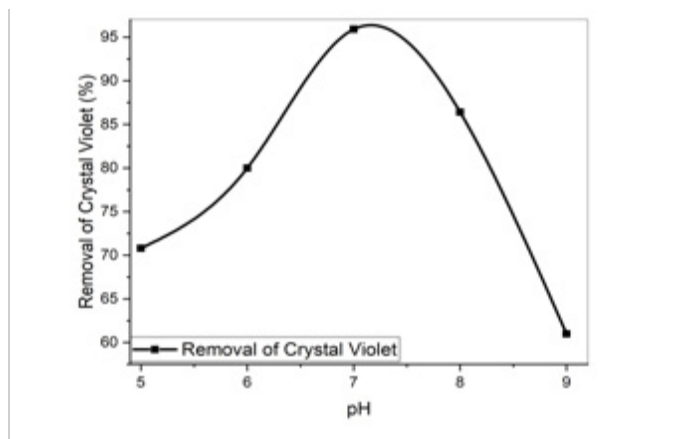


Figure 11: Effect of pH on Crystal Violet dye removal using PG-FeNPs.

### Effect of Initial Concentration of Aqueous Dye Solution (Ci)

Experiments are being conducted to investigate the influence of initial dye concentration on the removal of Crystal violet dye. The graph demonstrates that as dye concentration increases, dye absorption increases and dye removal decreases. An increase in the driving forces, or concentration gradient, is connected to an increase in dye absorption. The reduction in % removal for PG-FeNPs is owing to particle agglomeration and a reduction in the overall effective area of adsorption [23,24]. The % removal at greater doses decreases while the equilibrium adsorption increases. At lower concentrations, the interaction with the binding sites increases the removal percentage. The decrease in adsorption efficiency at higher concentrations is most likely due to adsorption site saturation.

### Effect of Temperature(K)

The adsorption of crystal violet by PG-FeNP at various temperatures revealed a reduction in adsorption ability when the temperature was raised. The adsorption process is influenced by temperature in two ways. The equilibrium capacity of the adsorbent for a certain adsorbate will change as the temperature changes. Batch tests were conducted at four constant temperatures: 303, 308, 313, and 318 K to study the

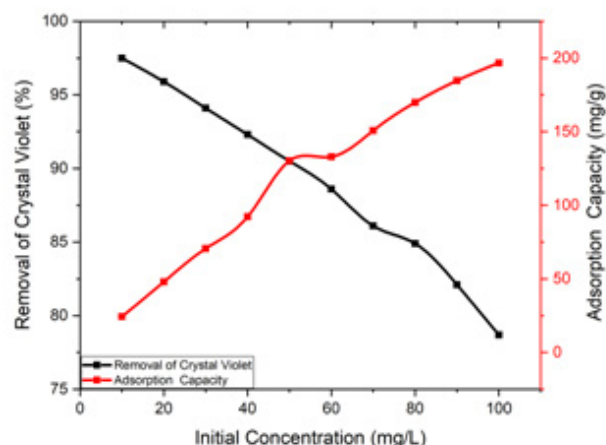


Figure 12: Effect of Initial Concentration of Aqueous dye solution vs % removal of dye vs adsorption capacity.

influence of temperature. As demonstrated, increasing the temperature improved the percentage removal from 98.0% to 99.2% for the initial concentration of 20mg/L. This implies that the adsorption process is exothermic.

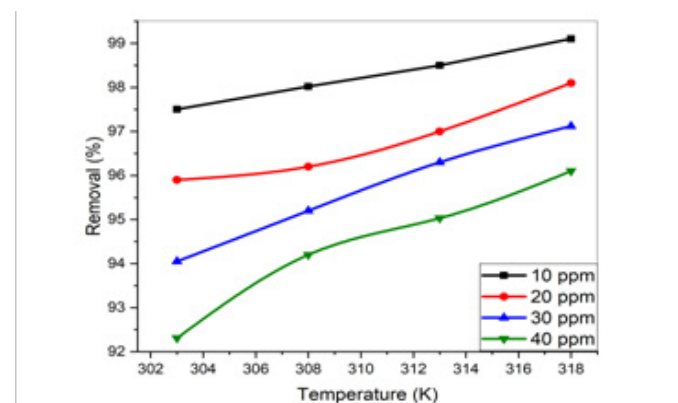


Figure 13: Effect of Temperature vs Crystal violet dye removal for four constant temperatures at 4 Dosages.

### Conclusion

The Effectiveness of Iron NPs synthesized from *Psidium guajava* in removal of crystal violet dye is studied. It is found that 99.2% removal efficiency is obtained by maintaining optimum parameters. Optimum parameters [contact time: 60 mins, dosage: 40mg/L, temperature of 318K, pH 7 and initial concentration] achieved are found to be safer, less energy consuming, and use minimal equipment. There is a future scope to study various textile dye removal using these materials and procedures. As the method is found to be less toxic, toxicity studies are to be performed to confirm it. The NPs via this route is found to be irregular and agglomerations are observed from SEM Images. The structure is found to be crystalline and polyphenol groups are found to play a key role in the reduction of iron. There are traces of Cl along with C and O which are due to the presence of precursor and flavonoids & water in the *Psidium guajava* NPs respectively.

### References

1. Pal G, Rai P, Pandey A (2019) Green synthesis of nanoparticles: a greener approach for a cleaner future. In Shukla AK, Iravani S (eds) Green synthesis, characterization



- and applications of nanoparticles. Elsevier. <https://doi.org/10.1016/B978-0-08-102579-6.00001-0>
- Xiao Z, Yuan M, Yang B, Liu Z, Huang J, et al. (2016) Plant-mediated synthesis of highly active iron nanoparticles for Cr (VI) removal: investigation of the leading biomolecules. *Chemosphere* 150: 357-364. <https://doi.org/10.1016/j.chemosphere.2016.02.056>
  - Chandrika K, Chaudhary A, Mareedu T, Sirisha U, Vangalapati M (2021) Adsorptive removal of acridine orange dye by green tea/copper-activated carbon nanoparticles (Gt/Cu-AC np). *Mater Today Proc* 44: 2283-2289. <https://doi.org/10.1016/j.matpr.2020.12.391>
  - Liu Y, Jin X, Chen Z (2018) The formation of iron nanoparticles by Eucalyptus leaf extract and used to remove Cr (VI). *Sci Total Environ* 627: 470-479. <https://doi.org/10.1016/j.scitotenv.2018.01.241>
  - Jeyasundari J, Praba PS, Jacob YBA, Vasantha VS, Shanmugaiiah V (2017) Green synthesis and characterization of zero valent iron nanoparticles from the leaf extract of *Psidium guajava* plant and their antibacterial activity. *Chem Sci Rev Lett* 6: 1244-1252.
  - Pan Z, Lin Y, Sarkar B, Owens G, Chen Z (2020) Green synthesis of iron nanoparticles using red peanut skin extract: synthesis mechanism, characterization and effect of conditions on chromium removal. *J Colloid Interface Sci* 558: 106-114. <https://doi.org/10.1016/j.jcis.2019.09.106>
  - Sahoo SK, Panigrahi GK, Sahoo A, Pradhan AK, Dalbehera A (2021) Bio-hydrothermal synthesis of ZnO-ZnFe<sub>2</sub>O<sub>4</sub> nanoparticles using *Psidium guajava* leaf extract: Role in waste water remediation and plant immunity. *J Clean Prod* 318: 128522. <https://doi.org/10.1016/j.jclepro.2021.128522>
  - Mokhtar MAM, Ali RR, Isa EDM (2021) Silver nanoparticles loaded activated carbon synthesis using *Clitorea ternatea* extract for crystal violet dye removal. *J Res Nanosci Nanotechnol* 3: 26-36. <https://doi.org/10.37934/jrnm.3.1.2636>
  - Fazlzadeh M, Rahmani K, Zarei A, Abdoallahzadeh H, Nasiri F, et al. (2017) A novel green synthesis of zero valent iron nanoparticles (NZVI) using three plant extracts and their efficient application for removal of Cr (VI) from aqueous solutions. *Adv Powder Technol* 28: 122-130. <https://doi.org/10.1016/j.apt.2016.09.003>
  - Shahwan T, Sirriah SA, Nairat M, Boyacı E, Eroğlu AE, et al. (2011) Green synthesis of iron nanoparticles and their application as a Fenton-like catalyst for the degradation of aqueous cationic and anionic dyes. *Chem Eng J* 172: 258-266. <https://doi.org/10.1016/j.cej.2011.05.103>
  - Devatha CP, Thalla AK, Katte SY (2016) Green synthesis of iron nanoparticles using different leaf extracts for treatment of domestic waste water. *J Clean Prod* 139: 1425-1435. <https://doi.org/10.1016/j.jclepro.2016.09.019>
  - Abdullah JAA, Eddine LS, Abderrhmane B, Alonso-González M, Guerrero A, et al. (2020) Green synthesis and characterization of iron oxide nanoparticles by *Phoenix dactylifera* leaf extract and evaluation of their antioxidant activity. *Sustain Chem Pharm* 17: 100280. <https://doi.org/10.1016/j.scp.2020.100280>
  - Farshchi HK, Azizi M, Jaafari MR, Nemati SH, Fotovat A (2018) Green synthesis of iron nanoparticles by Rosemary extract and cytotoxicity effect evaluation on cancer cell lines. *Biocatal Agric Biotechnol* 16: 54-62. <https://doi.org/10.1016/j.bcab.2018.07.017>
  - Huang L, Weng X, Chen Z, Megharaj M, Naidu R (2014) Green synthesis of iron nanoparticles by various tea extracts: comparative study of the reactivity. *Spectrochim Acta A Mol Biomol Spectrosc* 130: 295-301. <https://doi.org/10.1016/j.saa.2014.04.037>
  - Nagajyothi PC, Pandurangan M, Kim DH, Sreekanth TVM, Shim J (2017) Green synthesis of iron oxide nanoparticles and their catalytic and *in vitro* anticancer activities. *J Clust Sci* 28: 245-257. <https://doi.org/10.1007/s10876-016-1082-z>
  - Karpagavinayagam P, Vedhi C (2019) Green synthesis of iron oxide nanoparticles using *Avicennia marina* flower extract. *Vacuum* 160: 286-292. <https://doi.org/10.1016/j.vacuum.2018.11.043>
  - Demirezen DA, Yıldız YŞ, Yılmaz Ş, Yılmaz DD (2019) Green synthesis and characterization of iron oxide nanoparticles using *Ficus carica* (common fig) dried fruit extract. *J Biosci Bioeng* 127: 241-245. <https://doi.org/10.1016/j.jbiosc.2018.07.024>
  - Kanagasubbulakshmi S, Kadirvelu K (2017) Green synthesis of iron oxide nanoparticles using *Lagenaria siceraria* and evaluation of its antimicrobial activity. *Def Life Sci J* 2: 422-427. <https://doi.org/10.14429/dlsj.2.12277>
  - Gabal MA, Al-Harthy EA, Al Angari YM, Salam MA (2014) MWCNTs decorated with Mn<sub>0.8</sub>Zn<sub>0.2</sub>Fe<sub>2</sub>O<sub>4</sub> nanoparticles for removal of crystal-violet dye from aqueous solutions. *Chem Eng J* 255: 156-164. <https://doi.org/10.1016/j.cej.2014.06.019>
  - Jassal V, Shanker U, Gahlot S (2016) Green synthesis of some iron oxide nanoparticles and their interaction with 2-amino, 3-amino and 4-aminopyridines. *Mater Today Proc* 3: 1874-1882. <https://doi.org/10.1016/j.matpr.2016.04.087>
  - Priya R, Stanly S, Dhanalekshmi SB, Mohammad F, Al-Lohedan HA, et al. (2020) Comparative studies of crystal violet dye removal between semiconductor nanoparticles and natural adsorbents. *Optik* 206: 164281. <https://doi.org/10.1016/j.ijleo.2020.164281>
  - Selvaraj R, Pai S, Murugesan G, Pandey S, Bhole R, et al. (2021) Green synthesis of magnetic  $\alpha$ -Fe<sub>2</sub>O<sub>3</sub> nanospheres using *Bridelia retusa* leaf extract for Fenton-like degradation of crystal violet dye. *Appl Nanosci* 11: 2227-2234. <https://doi.org/10.1007/s13204-021-01952-y>
  - Sowjanya B, Sirisha U, Juttuka AS, Matla S, King P, et al. (2022) Synthesis and characterization of zinc oxide nanoparticles: its application for the removal of alizarin red S dye. *Mater Today Proc* 62: 3968-3972. <https://doi.org/10.1016/j.matpr.2022.04.576>
  - Golli R, Thummaneni C, Vangalapati M (2022) Green synthesis and characterization for the extraction of kaempferol from *Brassica oleraceavar. italica*—Antibacterial activity. *Mater Today Proc* 62: 3457-3461. <https://doi.org/10.1016/j.matpr.2022.04.280>